**Earthquakes and Structures**, *Vol. 8, No. 6 (2015) 1363-1386*
DOI: http://dx.doi.org/10.12989/eas.2015.8.6.1363 

# Strong ground motion characteristics of the 2011 Van Earthquake of Turkey: Implications of seismological aspects on engineering parameters

Kemal Beyen[*1] and Gülüm Tanırcan[2]

[1]*Department of Civil Engineering, Kocaeli University, Kocaeli, Turkey*
[2]*Kandilli Observatory and Earthquake Research Institute, Boğaziçi University, İstanbul, Turkey*

*(Received September 23, 2013, Revised June 19, 2014, Accepted March 6, 2015)*

**Abstract.** The October 23 2011 Van Earthquake is studied from an earthquake engineering point of view. Strong ground motion processing was performed to investigate features of the earthquake source, forward directivity effects during the rupture process as well as local site effects. Strong motion characteristics were investigated in terms of peak ground motion and spectral acceleration values. Directiviy effects were discussed in detail via elastic response spectra and wide band spectograms to see the high frequency energy distributions. Source parameters and slip distribution results of the earthquake which had been proposed by different researchers were summarized. Influence of the source parameters on structural response were shown by comparing elastic response spectra of Muradiye synthetic records which were performed by broadband strong motion simulations of the earthquake.

It has been emphasized that characteristics of the earthquake rupture dynamics and their effects on structural design might be investigated from a multidisciplinary point of view. Seismotectonic calculations (e.g., slip pattern, rupture velocity) may be extended relating different engineering parameters (e.g., interstorey drifts, spectral accelerations) across different disciplines while using code based seismic design approaches. Current state of the art building codes still far from fully reflecting earthquake source related parameters into design rules. Some of those deficiencies and recent efforts to overcome these problems were also mentioned.

Next generation ground motion prediction equations (GMPEs) may be incorporated with certain site categories for site effects. Likewise in the 2011 Van Earthquake, Reverse/Oblique earthquakes indicate that GMPEs need to be feasible to a wider range of magnitudes and distances in engineering practice. Due to the reverse faulting with large slip and dip angles, vertical displacements along with directivity and fault normal effects might significantly affect the engineering structures. Main reason of excessive damage in the town of Erciş can be attributed to these factors. Such effects should be considered in advance through the establishment of vertical design spectra and effects might be incorporated in the available GMPEs.

**Keywords:** thrust fault; seismotectonic; engineering parameters; the 2011 Van Earthquake; seismic design code; directivity effects; hanging wall effect; footwall effect

## 1. Introduction

*Corresponding author, Associate Professor, E-mail: kbeyen@kocaeli.edu.tr


http://www.techno-press.org/journals/eas&subpage=7 ISSN: 2092-7614 (Print), 2092-7622 (Online)

A thrust fault with a relatively shallow focal depth hit the Van region in the eastern part of Turkey on October 23 2011 (Fig. 1). Comparably small peak accelerations and sensible large displacements are not expected to cause extensive failure in the region. However, it caused widespread damage in flexible reinforced concrete buildings designed with nominal or high level of ductility. Extensive structural damage is located mainly in the town of Erciş and partially in the Van city center. It caused 644 fatalities, 252 injuries (AFAD 2011). In case of the earthquake resistant structural design, structural performances varied tremendously from poor to very good during the Van Earthquake. Possible reasons are arguable but characteristics of the earthquake rupture dynamics and their effects on structural design might be investigated from a multidisciplinary point of view.

In general, the large variability of structural damage is not simply reflections of low quality construction material, code incompliant design, inadequate reinforcement, poor detailing and workmanship but also inadequate values of the design parameters, which should be linked to some important features of the source to site wave propagation, but are generally ignored in the building codes.

Although the basic methodology for earthquake resistant ductile structural design and constructive details have been well established, there remains widespread misunderstanding of basic concepts, for instance, in the development and adaptation of design spectra into practice and other issues like effects of directivity and rupturing, regional propagation characteristics, characteristics of near and far field earthquakes that may contribute to poor practice. Results of such simulations with extant uncertainties on focal mechanism, seismic moment, fault plane etc. affect the values of the engineering parameters and the ground motion characteristics for the designer. It should be noted that instrumental intensity measurements (e.g., peak ground acceleration (PGA), peak ground velocity (PGV) and peak ground displacement (PGD) are preferred in earthquake hazard assessment by engineers rather than using indirectly estimated seismological parameters. (Heaton 1992).

For instance, near source factor, *N*, was included to represent near field conditions as a function of distance and the potential of the fault to produce large earthquakes in the revised version of the Uniform Building Code of 1997 (UBC 1997). It accommodates larger ground motions for large earthquakes either due to rupture directivity effect or near field effect (Somerville *et al*. 2000). Recorded ground motions in the near source regions during the 1994 Northridge Earthquake showed the acceleration exceeded 1.9 g, which also exceeds the UBC code spectrum (Somerville *et al*. 2000). The near source factor, *N*, becomes unity for the distance of 10 km and beyond for certain seismic source types. It is reported that ground motions recorded on the hanging wall block during the Northridge Earthquake were increased up to 50% larger than the median g values within the distances ranging 10 km to 20 km (Somerville *et al*. 2000). Such a finding shows that the near source factor needs to be studied more to verify such increments at larger distances on the hanging wall block of a thrust fault.

Additionally, it seems necessary to define new engineering parameters that may quantify the damage potential of destructive earthquakes in different tectonic settings. Current state of art in design practice and recently developed other engineering applications such as structural identification techniques, progressive damage identification techniques, active vibration control and structural health monitoring need performance assessment of existing structures relying inevitably on time history analysis. Seismic design codes prescriptively suggest using simulated earthquake recordings or scaled real earthquake components that should be well-matched with regional characteristics. Seismotectonic parameters can have strong influence on the quality of the simulation.

This study focuses on the effects of the seismology and earthquake physics on engineering design, some of the most common misunderstandings, misuse and common aspects of practice in assessment of the structural performance with emphasis on characteristics of the strong ground motion data recorded during the largest reverse mechanism earthquake in the instrumental period of Turkey.

## 2. Seismotectonic of the region

Eastern Turkey has a series of complex tectonic formations either by thrust or strike-slip faulting due to collision of Arabian plate and Eurasian plate with closing to each other at a rate of approximately 2.0-2.4 cm/yr (McClusky 2000). The October 23 2011 Van Earthquake (Mw 7.1) occurred in a broad region of convergence beyond the eastern extent of Anatolian strike-slip tectonics. Until the earthquake, faulting structures of the Van Region had not been well identified. Recent studies (Koçyigit 2013) have revealed that there are three different categories of faults falling in the Van region, strike-slip, thrust to reverse and oblique-slip normal. The Van Earthquake is one of the latest large magnitude earthquake triggered by an erosional reverse Van fault that lead to changes in continental settings of a complex area in Eastern Turkey. In the past, strike slip (e.g., the 1976 Ms: 7.5) and thrust faulting (e.g., the 1903 Ms: 6.3) earthquakes affected the region and caused heavy damage in the region. Epicentral locations of recent instrumentally recorded destructive earthquakes (Ms≥5.5) are shown in Fig. 1 (KOERI 2011).

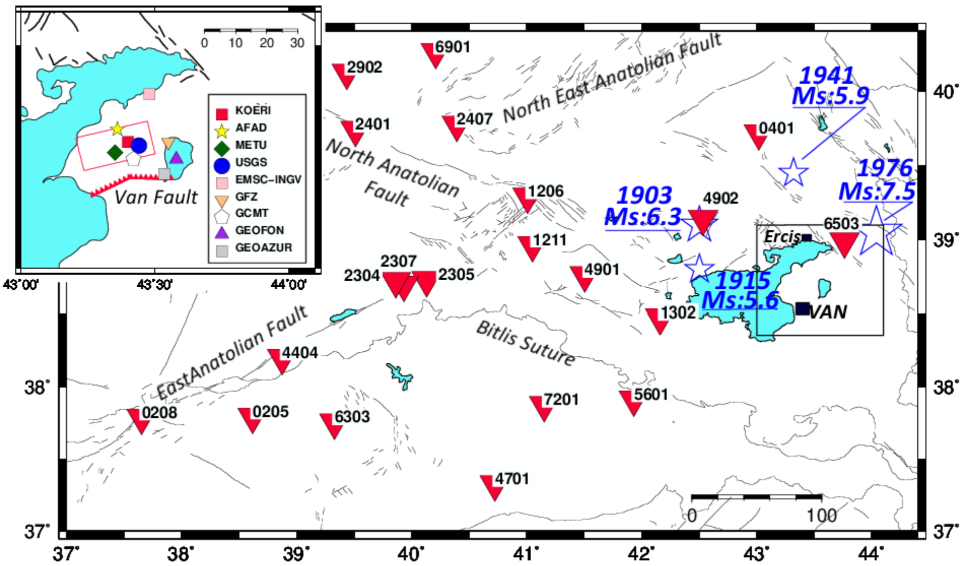


Fig. 1 Location of 22 regional strong ground motion recording stations of Disaster and Emergency Response Presidency (AFAD) used in the study. Various epicenter estimations of the 2011 main shock. A red box marks a single asperity projected to surface (Moro *et al*. 2014, Fielding *et al*. 2013). Van Fault with branches are also shown in red (after Emre 2011). Blue stars shows the epicenter of the events with Ms>5.5, black lines are active faults (MTA)

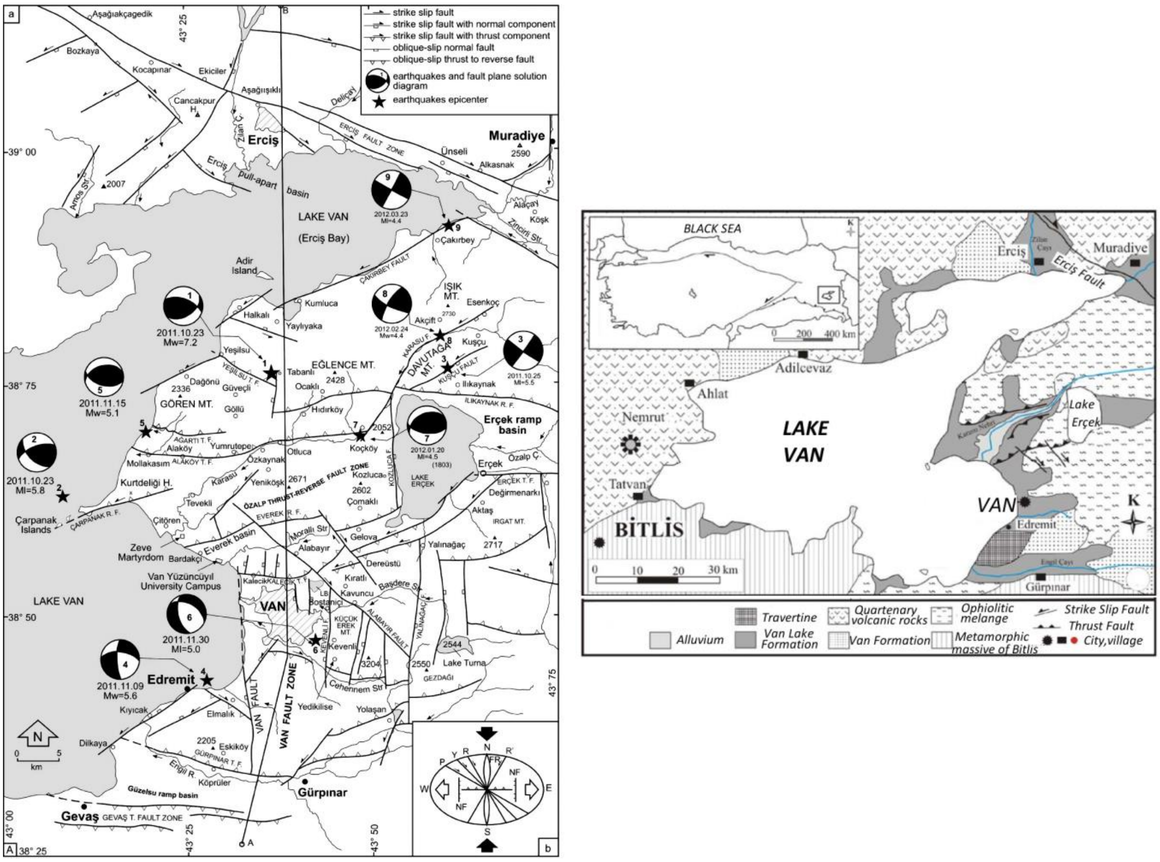


(a) (b)

Fig. 2 (a) Simplified seismotectonic map of the Van Earthquake region and pattern of the strike-slip faulting (Koçyiğit 2013) (b) Simplified geological condition of the Van region (from Okuldas and Üner 2013)

## 3. Geotechnical condition of the region

Because of intercontinental collisional tectonic activity in the eastern Mediterranean region, The Van Lake Basin was formed in the East Anatolian Plateau in late Miocene (Özkaymak *et al*. 2004, Şengör *et al*. 1979). The basement of the basin is formed with metamorphic massive of Bitlis, upper cretaceous ophiolites and tertiary aged marine sediments (Özkaymak *et al*. 2004). Different rock units and alluvial deposits are observed from the simplified geological map as shown in Fig. 2(b) (Okuldas and Üner 2013). The region includes metamorphic rocks belonging to the Bitlis Massive at the south, volcanic, volcano-clastic rocks accumulated at the west, and north part of the Lake formed by the old volcanoes called Nemrut, Süphan and Tendürek.

## 4. General seismological characteristic of the 23 October 2011 Van Earthquake

Several agencies declared various results for hypocenter and source parameters, which are compiled from the catalogues of KOERI, GCMT, USGS-NEIC and some other institutions (Table 1). From the coordinates listed in Table 1, possible epicenters are marked in Fig. 1 with the references. Recently improved values are also given in the parenthesis next to the preliminary ones in Table 1 as the values of the source parameters are clarified. It is officially stated that the October 23 2011 Van Earthquake with a moment magnitude, Mw, of 7.0 and seismic moment, Mo, of 2.09e22 dyne.cm occurred in the east part of Turkey. On the other hand, Kandilli Observatory and Earthquake Research Institute (KOERI) estimated the epicenter of the main shock near Tabanlı Village. Hypocentral depth was primarily estimated as 5 km and re-estimated as 26 km in their final report (Sarno *et al*. 2013), whereas the United States Geological Survey (USGS) computed the moment magnitude Mw 7.2 with a 16 km hypocentral depth using regional broadband waveforms. According to selected data catalogs, focal mechanisms and depths, which may have uncertainties, various slip inversion results as shown in Table 2 are obtained. As explained in the study of Husen *et al*. (2010), it is important to remember that the most accurate earthquake locations will be found from the most accurate velocity model. Therefore, care should be taken when using the results. Another important point for the designers is that, although the epicentral data is exactly same, two simulations of the USGS (listed as USGS1 and USGS2 in Table 1) with small differences in the values of the source parameters may show important influences in the seismic moments and magnitude, which are reference parameters for civil engineering usage.

Based on results of different institutions the hypocenter is certainly located onto the north of the Bitlis-Suture. Observed fault motion indicates that the Van Earthquake was generated by the Bitlis-Zagros Fault Zone (Fig. 2(a), (b)), where thrust mechanism mainly dominates the regional tectonics (Koçyiğit 2013). Focal mechanism solutions for the main shock, the distribution of aftershocks and a number of interferometric synthetic aperture radar (InSAR) studies correlate that the earthquake took place on a ENE-WSW striking, 45°-55° NW dipping reverse fault with a minor left-lateral component, consistent with the trend and location of the Van Fault' (Dogan *et al*. 2014, Akoğlu 2011).

Table 1 Reported source parameters of the Van earthquake by the research centers

| **Institutions** | **Latitude (°)** | **Longitude (°)** | **Depth (km)** | **Strike (°)** | **Dip (°)** | **Rake (°)** | **Mo (Joule)** | **Magnitude** |
|---|---|---|---|---|---|---|---|---|
| AFAD | 38.7578N | 43.3602E | 19.07 | | | | 2.09E15 | ML 6.7, Mw 7.0 |
| KOERI | 38.72N | 43.40E | 5, (26) | 241 | 51 | 58 | 6.4E19 | ML 6.6, Mw 7.1 |
| USGS1 | 38.71N | 43.44E | 20 | 255 | 50 | 74 | 6.4E19 | Mw 7.3 |
| USGS2 | 38.71N | 43.44E | 13, 16 | 241 | 51 | 58,50-70 | 5.6E19, (5.1E19) | Mw 7.1 |
| GCMT | 38.67N | 43.42E | 12, (15.4) | 248 | 36 | 60 | 6.4E19 | Mw 7.1, Ms 7.2 |
| GFZ | 38.72 | 43.55 | 10, (19) | 268 | 36 | 85 | 4.7E19,(5.8E19) | Mw 7.1 |
| EMSC | 38.86N | 43.48E | 10 | 248 | 53 | 64 | 6.86E19 | Mw 7.2 |
| INGV | 38.86N | 43.48E | 10 | | | | | Mw 7.3 |
| GEOFON | 38.67N | 43.58E | 15 | | | | | Mw 7.1 |
| GEO AZUR | 38.627N | 43.535E | 16, (23) | | | | | Mw 7.2 |
| METU(NERA) | 38.689N | 43.351E | 8-15 | 246 | 52 | 75 | 7.4E19 | Mw 7.1 |

Table 2 Various slip inversion results from researchers

| Author | Data | Input parameters | | Slip Inversion Results | | |
|---|---|---|---|---|---|---|
| | | Focal Mech. | Depth (km) | Max Slip (m) | Seismic moment (E19Nm) | Rupture time (sec) |
| Hayes 2011 | Teleseismic Waves | USGS 241/51/58 | 20 | 4 | 5.16 | 30 |
| Irmak 2012 | | 246/46/56 | 15 | 3.6 | 5.53 | 19 |
| Utkucu 2012 | | 255/50/73 | 16 | 5.5 | 4.6 | 11 |
| Gallovic 2013 | Strong Motion | 246/52/75 | 15 | 5.0 | 3.2- 4.0 | 12-25 |
| Moro 2014 | DInSAR+GPS | 252/50/74 | 15 | 3.8 | - | - |
| Fielding 2103 | InSAR+GPS teleseismic P- SH wave | 258/46/71 | 18 | 3.5 | 5.37 | 16 |

Teleseismic and strong motion waveform inversions (Hayes 2011, Irmak *et al*. 2012, Utkucu 2012, Gallovic *et al*. 2013), as well as InSAR and GPS studies (Fielding *et al*. 2013, Moro *et al*. 2014) yield different slip distributions on the fault plane. Number of slip patches and locations of them on fault plane differ in models. Maximum slip, seismic moment and rupture time varies, 3.5-5.5 m, 3.2 E16 -5.5 E16 Nm, 11-30 sec, respectively, as shown in Table 2.

## 5. Strong ground motion recordings and their characteristics

The National Strong Ground Motion Network (NSMN) is operated by the (AFAD) in Turkey. Regional stations located within a distance of about 40 km to 590 km from the epicenter of the main shock. Each station is equipped with three component force-balance accelerometers located at the base of state houses with 2-3 stories. Locations of national and regional stations are given with station codes and names in Fig. 1. List of twenty-two stations of national strong ground motion network that recorded main shock is tabulated in Table 3.

Because the near fault region is subjected to large velocity pulses recordings may additionally show artificial residual displacements. Precise data processing is inevitable particularly for the epicentral stations and integration of the accelerogram definitely affects the resultant velocity and displacement. High-pass zero phase bi-directional acasual Butterworth filter at 0.05 Hz is applied after several test works. Iwan's method (option 1) is also adopted to correct the baseline distortions (Boore 1999). Fig. 3 shows the displacement time histories for the three orthogonal components. It appears that, ground motion amplitudes are attenuated gradually as the stations are becoming far from the epicenter. The oblique characteristic may generate regular energy distribution in two horizontal components, which yield so far close frequency content at the corresponding times. Therefore, similar displacement shapes synchronized with the time in both horizontal directions are observed in Fig. 3. Even vertical components received similar built up characteristic. Strong motion measurements of Van and Erciş stations in the epicenter region are not available due to a technical malfunctioning.

The nearest strong motion station to the epicenter of the main shock is Muradiye with the

Table 3 PGA values and site information for the Van Earthquake (AFAD 2011)

| Stations | | Peak Ground Acc. (gal) | | | Epicentral Distance *Repi* (Km) | Joyner-Boore Dist. $R_{JB}$ (Km) | $V_{S30}$ (m/sn) |
|---|---|---|---|---|---|---|---|
| **Code** | **Name** | **NS** | **EW** | **UD** | | | |
| **6503** | muradiye | 178.5 | 168.5 | 75.5 | 46.6 | 19.5 | 293 |
| **4902** | muş | 44.3 | 55.75 | 25.5 | 93.2 | 74.25 | 311 |
| **1302** | bitlis-dsi | 89.66 | 102.24 | 35.51 | 116 | 82.8 | Alluvium* |
| **401** | agri | 18.45 | 15.08 | 7.21 | 121 | 114.0 | 295 |
| **5601** | siirt | 9.90 | 9.16 | 7.04 | 158 | 124.48 | Alluvium* |
| **4901** | muş | 10.3 | 6.86 | 4.64 | 170 | 138.2 | 315 |
| **1211** | bingol_solhan | 4.58 | 4.19 | 2.46 | 211 | 180.38 | 463 |
| **1206** | bingol_karliova | 7.52 | 11.08 | 4.65 | 222 | 194.07 | Stiff* |
| **7201** | batman | 8.29 | 8.58 | 3.74 | 223 | 188.86 | 450 |
| **2307** | mardin | 2.0 | 1.90 | 1.58 | 284 | 274.13 | Stiff* |
| **2305** | elazig_beyhanioo | 1.20 | 1.19 | 0.99 | 289 | 256.92 | Stiff* |
| **2307** | elazig_palu | 2.11 | 1.64 | 1.72 | 307 | 274.13 | 329 |
| **2304** | elazig_kovancilar | 1.45 | 1.66 | 1.20 | 313 | 280.02 | Alluvium* |
| **2407** | erzincan_tercan | 2.37 | 3.43 | 2.26 | 289 | 264.72 | 320 |
| **2401** | erzincan | 1.53 | 1.29 | 0.71 | 358 | 331.84 | 314 |
| **6901** | bayburt | 1.35 | 1.14 | 1.27 | 327 | 306.17 | Stiff* |
| **2902** | gumushane_kelkit | 1.05 | 0.88 | 1.25 | 378 | 354.76 | Alluvium* |
| **6303** | urfa_siverek | 2.0 | 3.06 | 0.96 | 378 | 342.91 | Alluvium* |
| **4404** | malatya_poturge | 0.99 | 0.99 | 0.94 | 405 | 370.42 | Stiff* |
| **205** | adiyaman_kahta | 2.96 | 2.7 | 1.64 | 437 | 401.87 | Alluvium* |
| **208** | adiyaman_golbasi | 1.12 | 0.74 | 0.35 | 521 | 484.15 | 469 |
| **4609** | KMaraş | 1.74 | 2.18 | 0.96 | 590 | 552.79 | 317 |

*$V_{S30}$ is determined as a result of field observation

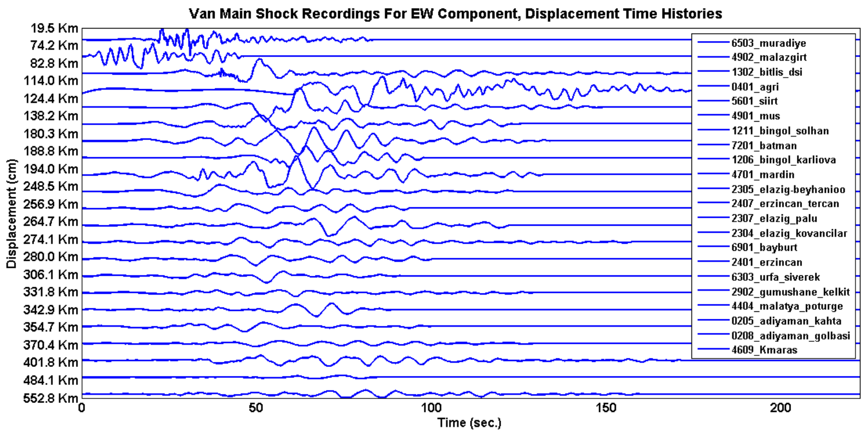


Fig. 3 NS, EW and vertical component displacements recorded at the 22 regional stations on 23 October 2011 from the closest to far distances

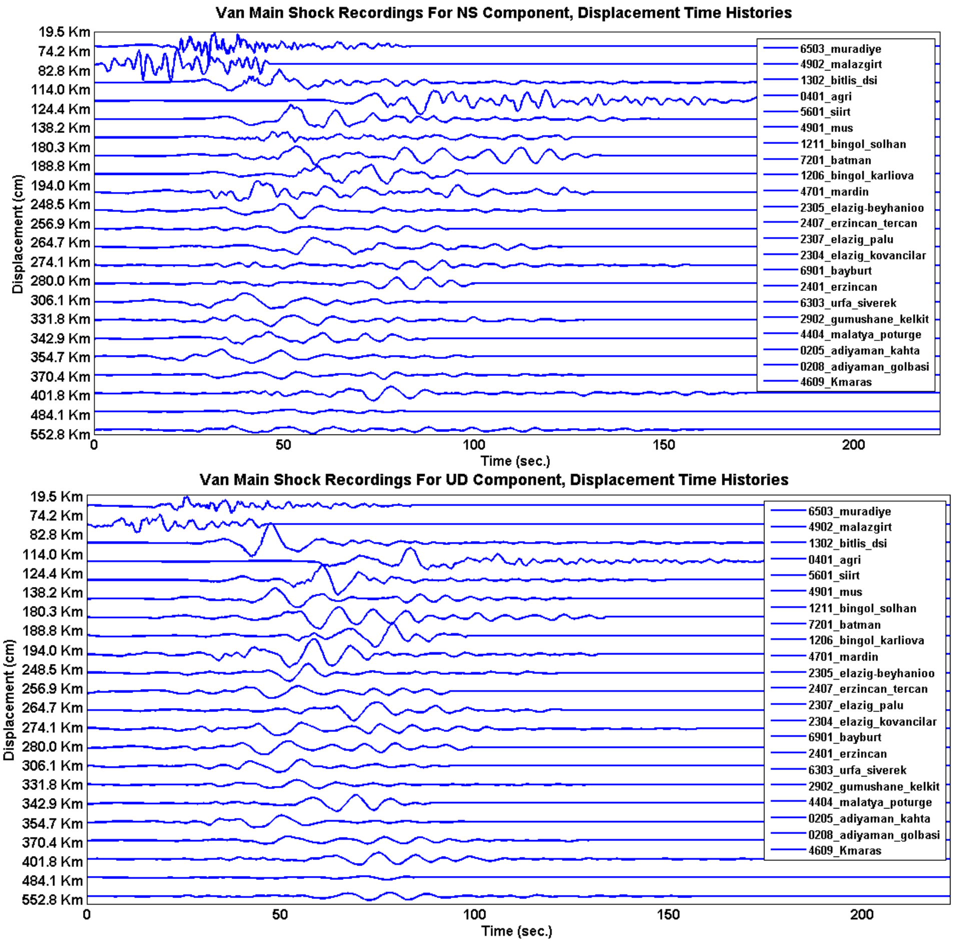


Fig. 3 Continued

distance to the epicenter approximately same as that of Erciş. Consequently, if the effect of the site characteristics is similar or ignored, it can be assumed that both towns received approximately same ground motion. Such a deduction appears reasonable when aftershock simulations and discussions of Gallovic *et al*. (2013) are considered among several simulation-based research groups. They developed a broadband strong motion model with different source models to illustrate broad variability in possible rupture propagation. Distribution of simulated values reaches up to 0.9 g and 100 cm/sec for PGA and PGV respectively in the epicenter region. Predicted values of Muradiye are compatible with the recordings (0.15 g). PGA value at Erciş with 0.15 g (PGV values around 20 cm/sec) appears to correlate well with the recorded PGA value.

### *6.1 Comparison with Ground Motion Prediction Equations (GMPEs)*

Limitations of the prediction equations in terms of magnitude, distance ($r_{jb}$) and types of faulting (reverse/oblique) are considered as major parameters to select suitable GMPEs. For instance, influence of the fault mechanism shows much variation among models. From recently

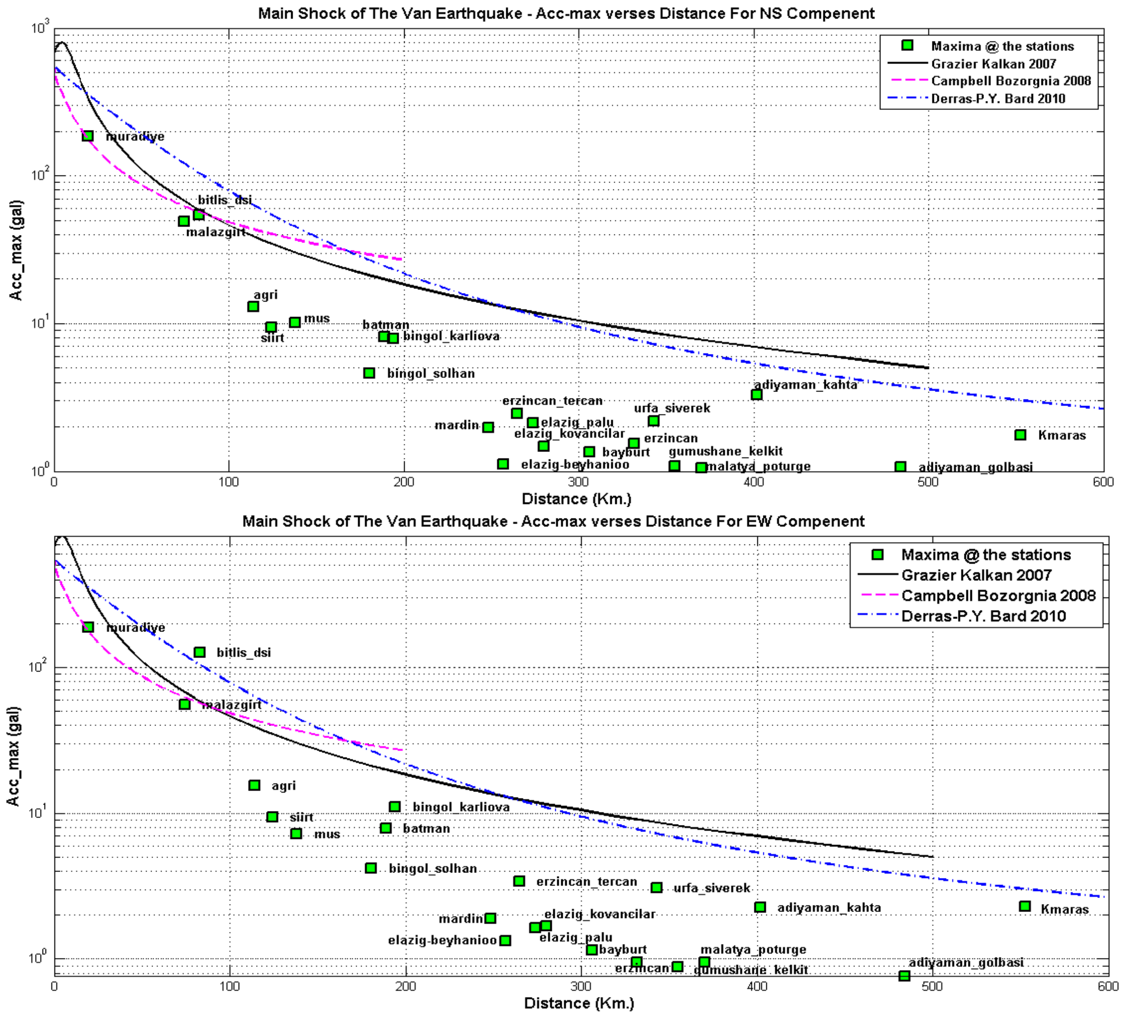


Fig. 4 For the 23 October 2011 Van Earthquake, estimations of the PGA distance attenuations in vertically logarithmic scale for NS and EW components

developed available set of GMPEs, which are valid for estimating ground motions for far distances, predictive models of Grazier and Kalkan (2007), Campbell and Bozorgnia (2008), Derras and Bard (2012) were adopted for the comparison of the predicted and measured strong ground motion parameters as shown in Fig. 4.

The distinguishable difference of the ground motions at two sides of the thrust fault may be emphasized by the comparison of maxima of the main shock recordings as shown below in Fig. 4. The ground motion of the hanging-wall side station Muradiye (station code: 6503) with relatively high peaks and many stations within 100 km to 200 km on the foot-wall side show thrust fault characteristic with lower acceleration peaks around 3-4 gal. The footwall side station Bitlis-dsi is exceptional and is located on the front of the rupture directivity at a closest ($r_{jb}$) distance of 83 km from the hypocenter of the main shock. It has a particular directivity characteristic with a large PGA value of 126 gal in EW (fault parallel) and 54 gal in NS direction (fault normal) in contrast to small PGA values as expected as a characteristic for the foot wall side.

Another regional station Muş at a closest (***r**$_{jb}$*) distance of 138 km from the fault recorded PGA value of 10 gal in NS and 7 gal in EW direction. The largest peak value is occurred in the fault normal component, NS and it might be also explained by soil characteristics due to site responses. PGA estimation with acceptable aleatoric uncertainty might fulfill the missed maxima of the malfunctioning stations in Van and Erciş close to the epicenter region as well as other locations. It is found that comparison of proposed GMPEs is not well matched with each other. However, except Bitlis-dsi, which took rupture directivity effect in EW direction, Grazier-Kalkan, and Campbell-Bozorgnia models predict almost close peak values for the stations in the first 100 km and Derras-Bard overestimates the peak values for up to 100 km. When considering larger distances, it is found that trends of proposed models are rarely above the recorded ones; however, overestimation makes the values conservative for engineering design. When the distance to the fault rupture increases, estimated PGA values become similar as seen in Fig. 4. For the town of Erciş, PGA values may be similar to Muradiye and the city of Van should be lower than the estimated value of Muradiye due to the footwall characteristic.

### *6.2 Characteristics of the regional elastic response spectra*

Design spectra in Turkish earthquake code, (TEC 2007), are defined with respect to seismic zone and site classes. Code-based design spectra may be also modified in accordance with the preferred performance level of the structure. Seismic load response modification factor, $Ra(T)$ shall be determined through the use of a structural behavior factor, $R$, and fundamental period of a structure, $T$. For a typical flexible building, fundamental period will be greater than $T_a$. Then the modified design value becomes $A(T)/R$ for elastic non-collapse mechanisms at the desired seismic performance level. In the Fig. 5, dashed-lines with square, diamond and triangle stand for 1 (non-ductile), 4 and 8 (ductile) for the modification factor, $R$. During the Van Earthquake, in the epicenter region, earthquake response of ground motions exceeded the code based modified response spectra. Fundamental periods of many buildings in the region correspond to structural period between 0.3 sec and 1.0 sec where they enter to the elasto-plastic range as offered by the modified code spectra.

A web-based application interface of the PEER is also utilized to estimate NGA response spectra on the basis of empirical models of Abrahamson and Silva (2008) (A&S), Boore and

Table 4 Simulated and observed spectral accelerations at three stations calculated by Zengin and Caktı (2014), Muradiye station by Gallovic *et al*. (2013). GM stands for geometric mean of two horizontal components

| **Stations** | Muradiye (6503) | | | | | | Bitlis-dsi (1302) | | Malazgirt (4902) | |
|---|---|---|---|---|---|---|---|---|---|---|
| **Spectral Periods-T (sec.)** | 0.5 | | | 1 | | | 0.5 | 0.5 | 1 | 0.5 |
| **Components** | NS | EW | GM | NS | EW | GM | NS | EW | GM | NS |
| **Observed S.A. (cm/sec$^2$)** | 544 | 369 | 450 | 544 | 369 | 450 | 544 | 369 | 450 | 544 |
| **Simulated S.A (cm/sec$^2$) (Gallovic *et al*. 2013)** | 410 | 210 | 293 | 410 | 210 | 293 | 410 | | 210 | |
| **Simulated average S.A. (cm/sec$^2$) (Zengin and Caktı 2014)** | 300 | | | | | | 300 | | | 300 |

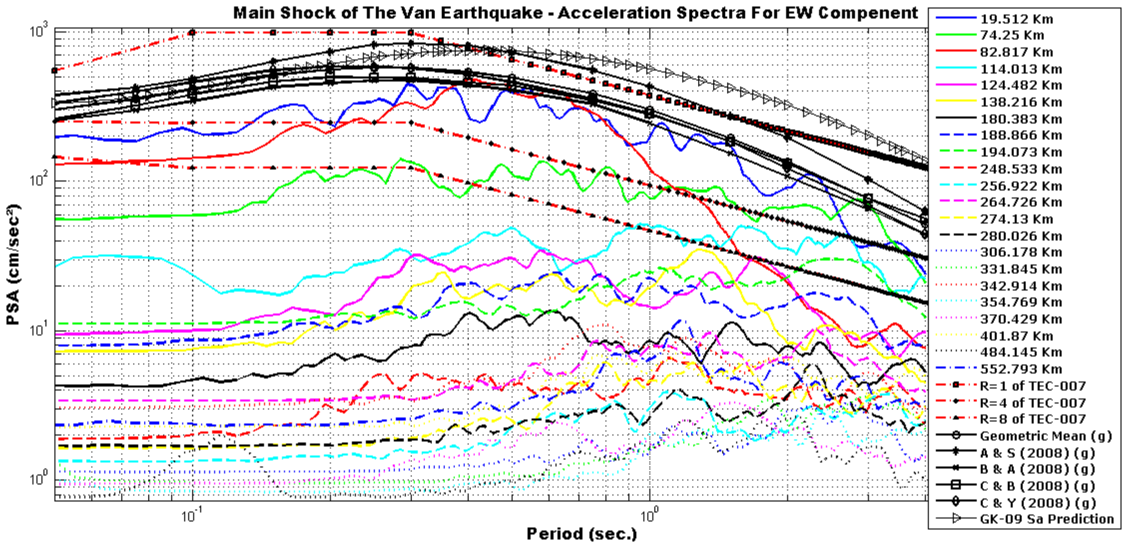


(a)

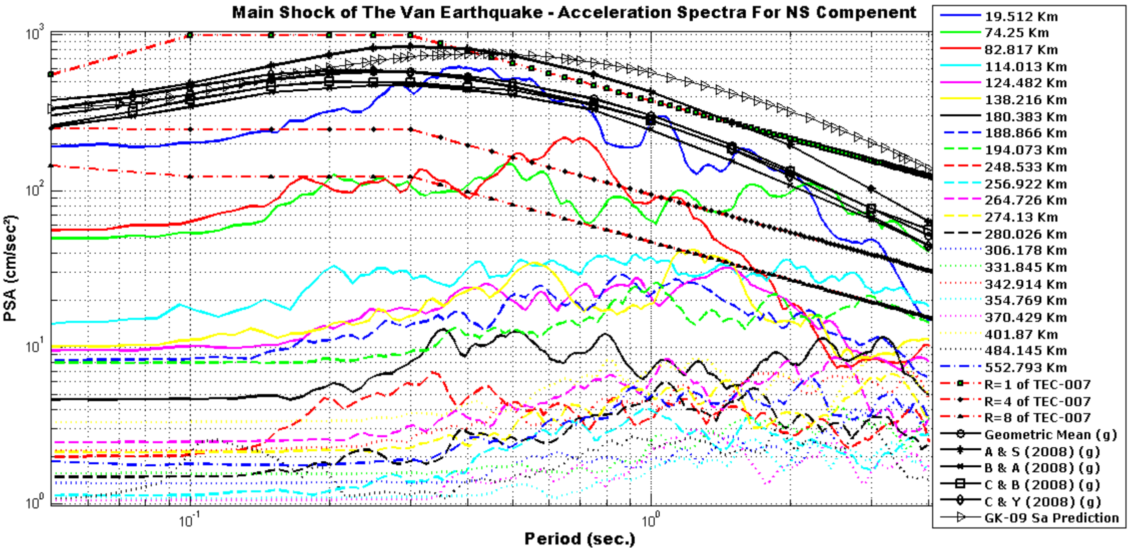


(b)

Fig. 5 PSA plots of the main shock data recorded by 22 stations in the region and the elastic acceleration design spectra of the TEC with different *R*-values (*R*=1, 4, 8) together with NGA spectra of A&S, B&A, C&B, C&Y and GK09 for horizontal components, (a) EW(FP) and (b) NS(FN)

Atkinson (B&A), Campbell and Bozorgnia (2008) (C&B), Chiou and Youngs (2008) (C&Y) and empirical model of Gülkan and Kalkan (2004) (GK09). Empirical models of GMPE spectra of PEER are estimated from the collection of ground motions of major shallow crustal earthquakes all over the world whereas the prediction model of the GK09 was derived from the database compiled from the earthquakes of Turkey with Mw magnitude ranging between 4.0 and 7.4 occurred between 1976 and 2003. As seen from Fig. 5, if estimated GMPE spectra are plotted together with the spectra of the main shock recordings, it is seen that the GMPE spectra broadly well envelope the spectra of the recordings and it shows conservative appearance for seismic design of structures. The current TEC design spectrum is also on the conservative side for structures with short fundamental periods when compared with the predictions.

Prediction of the Van Earthquake strong ground motions in the epicentral area were performed by two groups. Gallovic *et al*. (2013) used four rupture models for estimation of ground motions at Muradiye station. Zengin and Caktı (2014) used one rupture model to estimate ground motion time histories at selected six stations within 100 kms. From an engineering design point of view, for instance for structures with the fundamental periods of 0.5 sec and 1 sec, synthetics and observed averages are summarized in Table 4 for spectral acceleration. Each estimation holds significant discrepancy in between synthetics and target data. For instance, as a typical engineering application, if the synthetic was used as a design force for a structure with a typical fundamental period of 0.5 sec, it is clear that the demand of the main shock would be 1.5 times, 1.6 times and 2.7 times larger than the estimated design forces for such typical structures of Muradiye, Malazgirt and Bitlis-dsi, respectively. Loss of lives will be the most devastating hazard beside the loss of property, which can be rebuilt. Inclusion of the fault rupture directivity effect in probabilistic hazard analysis will certainly develop the results for instance for Bitlis-dsi in this case and for sites located near active faults.

### *6.3 Directivity effects*

Directivity effect is a phenomenon observed quite often during rupturing of the main fault. It manifests that the earthquake ground motion in the direction of rupture propagation is more severe than in any other directions. Top layers of a thrust fault covered by rock formations in the crustal part may not rupture all the way up to the surface due to condition of tectonic settings. Therefore, it cannot be traced on the ground surface. In case of such situation important amount of energy release occurs in the high frequency range (in the low periods) and soil layers cannot robustly filter out the high frequency components in ground tremors. Such an energy dominant component can be seen in the frequency content of the earthquake recordings. Controversially, open ground surface cracks of the causative fault may show filtering effect of soil layers during the propagation of rupture. The top of the ruptured Van Fault is covered by soft soils at the closest station of recordings in a shallow formation and the dominant period of soil at this location varies 0.4 sec to 0.6 sec. The response spectra of all recordings for five percent critical damping are shown in Figs. 6 through 8. Shapes of the response spectra change with respect to fault normal and fault parallel components. The rupture propagates at an almost constant velocity along the fault plane and it manifests the directivity effect in the NS (FN) component of the recording for Muradiye station with a dominant peak PSA, 600 cm/sec$^2$ at the period of 0.4 sec and drops down approximately at 2 sec. In the fault parallel (EW) direction, station Muradiye has many peaks up to 400 cm/sec$^2$ with the periods ranging from 0.1 sec to 2.5 sec. On the other hand, ground motion of Bitlis-dsi gives small PSA peaks with maximum value of 200 cm/sec$^2$ with the periods up to 1.5 sec in the NS (FN) component, but in the EW (FP) component, it yields one single sharp PSA peak at 0.4 sec, which is larger than the peaks of the closest station, Muradiye.

In the elastic PSV spectra as shown in Fig. 7, Muradiye shows many large peaks oscillating about average velocity of 30 cm/sec for the fault normal (NS) and fault parallel (EW) components at about 0.5 sec, 1 sec, 1.1 sec and 2 sec. Such a nearly similar propagation characteristic that is observed in both major directions but with different peak values reflects propagation of the progressive rupture. Bitlis-dsi in front of the rupture direction at a Joyner-Boore distance ($\boldsymbol{r_{jb}}$) of 83 km,

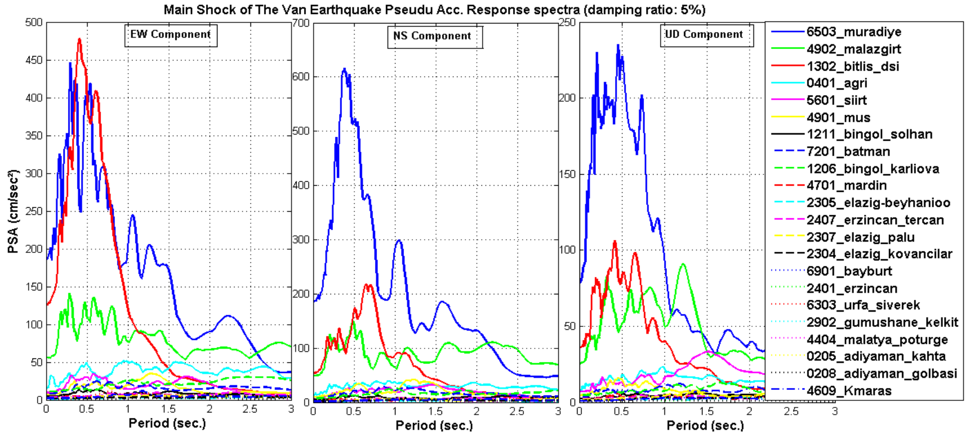


Fig. 6 PSA plots of the main shock data recorded by 22 stations in the region for EW (FP), NS (FN), and vertical components respectively from left to right

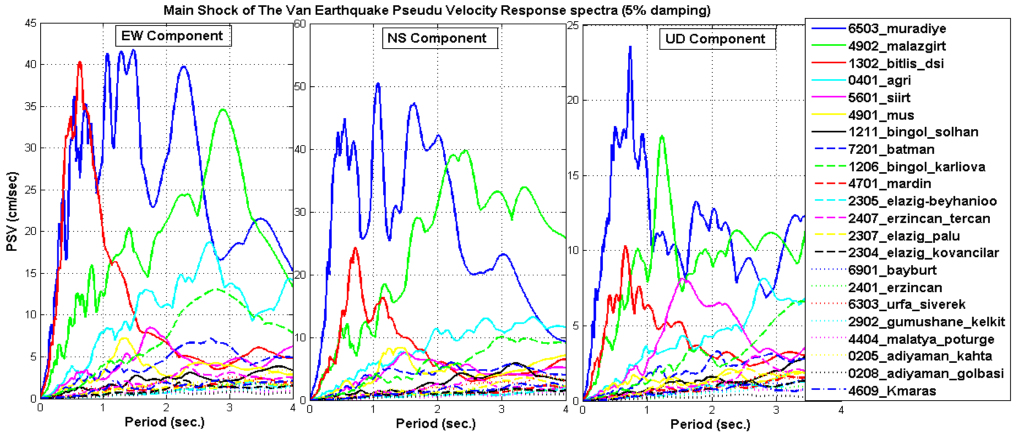


Fig. 7 PSV plots of the main shock data recorded by 22 stations in the region for EW (FP), NS (FN), and vertical components respectively from left to right

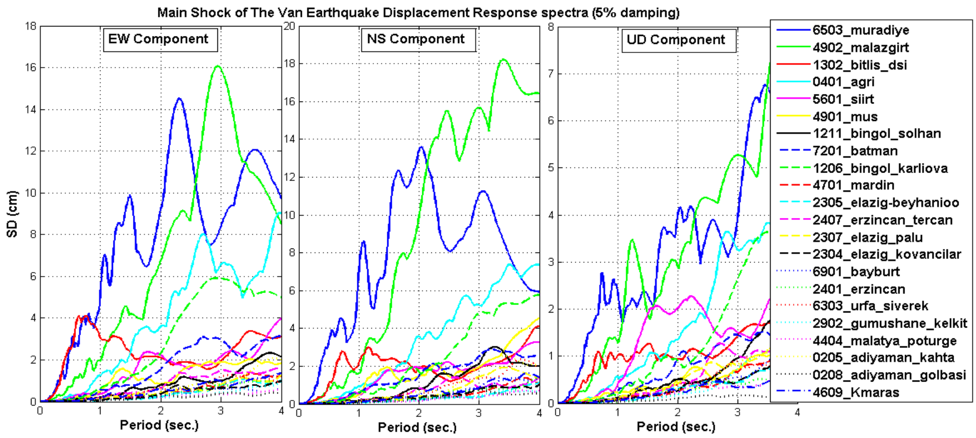


Fig. 8 SD plots of the main shock data recorded by 22 stations in the region for EW (FP), NS (FN), and vertical components respectively from left to right

yielding single PSV peak at 0.6 sec, almost close to the Muradiye. It is strong indicator declaring rupturing directivity effect for the city of Bitlis-dsi with single spectral broad band peak larger than Muradiye in both velocity and acceleration spectra for the fault parallel (EW) direction. Controversially fault normal (NS) component have larger period band peaks at specific peak periods such as 0.5 sec, 1 sec and 2 sec. In the FN (NS) direction, Bitlis-dsi has almost small peak values in the PSA and PSV spectra.

For the vertical component, Muradiye recorded the most prevailing one with broad band peak characteristics in PSA and PSV spectra. In spectral displacements, Muradiye has almost dominant peaks in both FN (NS) and FP (EW) components with the periods up to 2 sec at where the city of Bitlis-dsi starts to become dominant. For the vertical (UD) component, peaks of the closest stations are interchangeably varying in the displacement spectra as seen in Fig. 8.

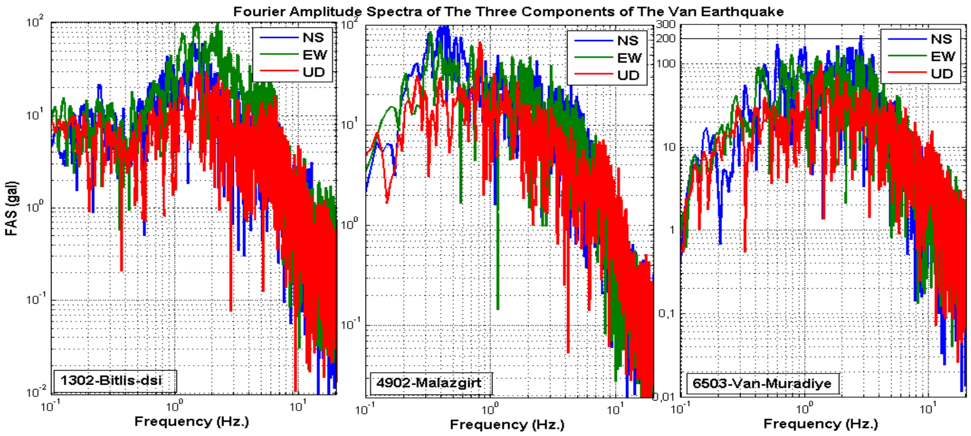


Fig. 9 FAS of the acceleration ground motions recorded by comparatively closest three stations, Bitlis-dsi, Malazgirt and Muradiye from left to right

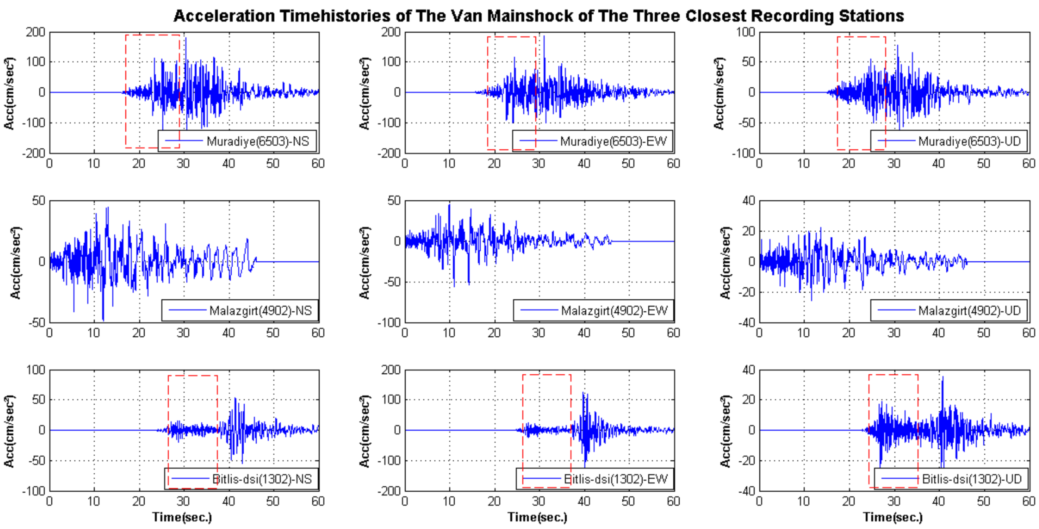


Fig. 10 Acceleration time histories with three components for Muradiye, Malazgirt and Bitlis-dsi recording stations. Recordings are marked for the first segment of multiply scattered waves

Fig. 9 shows the Fourier amplitude spectra (FAS) of the acceleration ground motions recorded by comparatively closest three stations. Spectra are smoothed by filtering with Savitzky-Golay smoothing filter. Filter with polynomial order 2 and time frame of 3 sample are used for removing the high frequency oscillations or noise within the given time frame. Peaks of the horizontal components in FAS seem almost similar for all stations including Muradiye, except the station Bitlis-dsi with particularly larger values of the fault rupture direction (EW) in a large frequency band between 0.3 and 7 Hz.

Sixty-second time window of the acceleration time histories with three components for Muradiye, Malazgirt and Bitlis-dsi recording stations are plotted in Fig. 10. The seismic energy of a large coda waveform pulse package verifies the effect of forward directivity in the beginning of the ground motion time history shortly before the initiation of the second rupture. Recordings are also marked for the first segment of multiply scattered waves with dashed red box in the figure. This behavior is mostly observed for the strike-slip faults. In contrast, depending on the rake angle, reverse and oblique faults might have this unique characteristic in both FN and FP components because of complex combination of rupture mechanism as observed in this case. Muradiye and Bitlis-dsi at the rupture front show such rupture propagation characteristic perceptibly in three directions. Malazgirt as the station with no pre-event set and receiving back propagations does not show such peculiarity. Particularly, it is well known fact that in near-source regions ground motions with large amplitude, short duration pulse content has potential to create excessive damage in the residential regions as experienced in Erciş. Forward-directivity effect, which is observed in the near source region, may become observable characteristic for the far field regions for the earthquakes that have reverse-oblique characteristics if the magnitude and the rupture duration as well as the number of the ruptured segments (therefore multi-phase earthquake) increase. Comparatively closest regional hanging-wall station Muradiye possibly recorded multiple rupture as shown with two distinctive ground motions in the components. Records of Bitlis-dsi in the front of the rupturing directivity also show such a characteristic event with three components and vertical one with exceptionally two coda shape waveforms reflects the multiple rupturing process of the main earthquake. If the EW (FP) component acceleration value of Bitlis-dsi is compared with NS (FN), another indicative characteristic is seen with peak acceleration value of 126 cm/sec$^2$ close to that of the source station Muradiye. This condition might be explained by the consistency of the slip direction of the fault plane and the direction of the rupture propagation in the center of energy release to the station. Although recordings of hanging wall station Malazgirt was limited to about 45 sec, long duration single large size coda waveform ground motion indicates the occurrence of backward directivity characteristics, which has comparatively lower amplitudes in all directions. Furthermore, vertical acceleration value of 35 cm/sec$^2$ recorded at the station Bitlis-dsi (83 km of $\boldsymbol{r_{jb}}$) larger than 25 cm/sec$^2$ of Malazgirt (74 km of $\boldsymbol{r_{jb}}$) might be another clue of the peculiarities associated with the earthquake source characteristic.

Observed peak ground velocities at Muradiye (19.5 km), Malazgirt and Bitlis-dsi are computed as 25.48 cm/sec, 12.7 cm/sec and 5.76 cm/sec for NS (FN) component and 15.8 cm/sec, 10.8 cm/sec and 11.01 cm/sec for EW (FP) component, respectively (Fig. 21). Comparisons of the peak velocities yield that the NS (FN) components have larger values than the EW (FP) components, except for the station Bitlis-dsi. Fault parallel component of Bitlis-dsi is remarkably two times larger than the peak value of the fault normal component. Even though the Bitlis-dsi station is located approximately 83 km away from the center of energy release, forward directivity effect is evident with the help of recordings. Peak displacements of the Fig. 11 show another distinguishable characteristic for the causative earthquakes with reverse fault. If the values of the first nine stations within the distances of 200 km are compared, it can be easily seen that the peak displacements are gradually reduces to a stable value. Such peculiarity is seen strongly in vertical components.

Very low frequency waves cannot attenuate easily and they will be subjected to be overlapped with the sub-events. Controversially, high frequency waves are attenuated in short time and lets the high-frequency waves of other sub-events to be distinguished visually in Time-Frequency analysis. Based on this point, recordings are high pass filtered at 2 Hz. only to see the high frequency wave characteristic of the sub-events in case of any possible multi-rupturing. Velocity time histories and corresponding spectrograms are plotted together in Fig. 12. In order to achieve high frequency-time resolution, Fourier analysis window is taken suitable. Wide band spectrogram is resulted as seen in Fig. 12, which holds individual site frequencies appearing as vertical lines up to Nyquist frequency of 50 Hz. Top three plots of the Fig. 12 shows that the closest hanging-wall station Muradiye reflects well-built multi-rupturing characteristic especially in FN (NS) component. The oblique system generates the regular energy distribution in two horizontal components, which yield so far close frequency content at the corresponding times. Such progressive ruptures are also seen at the same instants with energy increase in frequencies up to 30-40 Hz from the spectrograms. Although Malazgirt is a far-field station fading velocity pulse packages in the fault-normal direction it reflects a similar energy distribution. The station Malazgirt with comparatively lower amplitudes of a longer duration of a single large size code shape ground motion reflects backward directivity effect as compared with Fig. 10. It is understood that due to eastward rupture propagation and variations of the locations of subevents, amplitude of the second arrival might be weaker than the first arrival at Muradiye and Muradiye became backward station just like Malazgirt for further ruptures. The station Bitlis in the direction of the fault rupture shows strong progressive rupture characteristic in all components of the recordings. Reverse-oblique mechanism under rupture directivity effect is manifested in all components but especially vertical one reflects the up and down tilts with increasing energy up to 50 Hz.

## 7. Discussions

For critical structures such as bridges, dams, large flexible structures, etc., it is common to analyze the structure deterministically based on an estimated earthquake size and location like maximum credible earthquake (MCE) or safety evaluation earthquake (SEE). For instance, the SEE may be assessed based on following parameters: (a) earthquake size (magnitude and seismic moment), (b) closest distance to the center of energy release, (c) response spectra for the site, and (d) free field ground motion histories recorded or estimated at or near the construction site. Among these critical parameters, seismic moment, magnitude and the distance are very dependent on the results inferred from the seismological studies. Moreover, if there is no observation station close to the construction site and synthetic seismogram is considered for design. Available outcrop motion or the most comparable observed base rock data and estimated source parameters such as the type of fault, propagation path and local site condition become other control parameters; inversions are performed to regenerate the target spectrum compatible time histories. Simulation of synthetic ground motions will strongly depend on the quality of the estimated values of the seismological parameters where the values of source parameters are not directly accessible by measurement.

Mechanical complexity of the seismogenic process on the fault source and the geological complexity along the propagation paths are certain sources affecting and controlling the rupture characteristics and site responses. Simulation models and methods from very first source model to the last step numerical structural model considering all the uncertainties of the earthquake

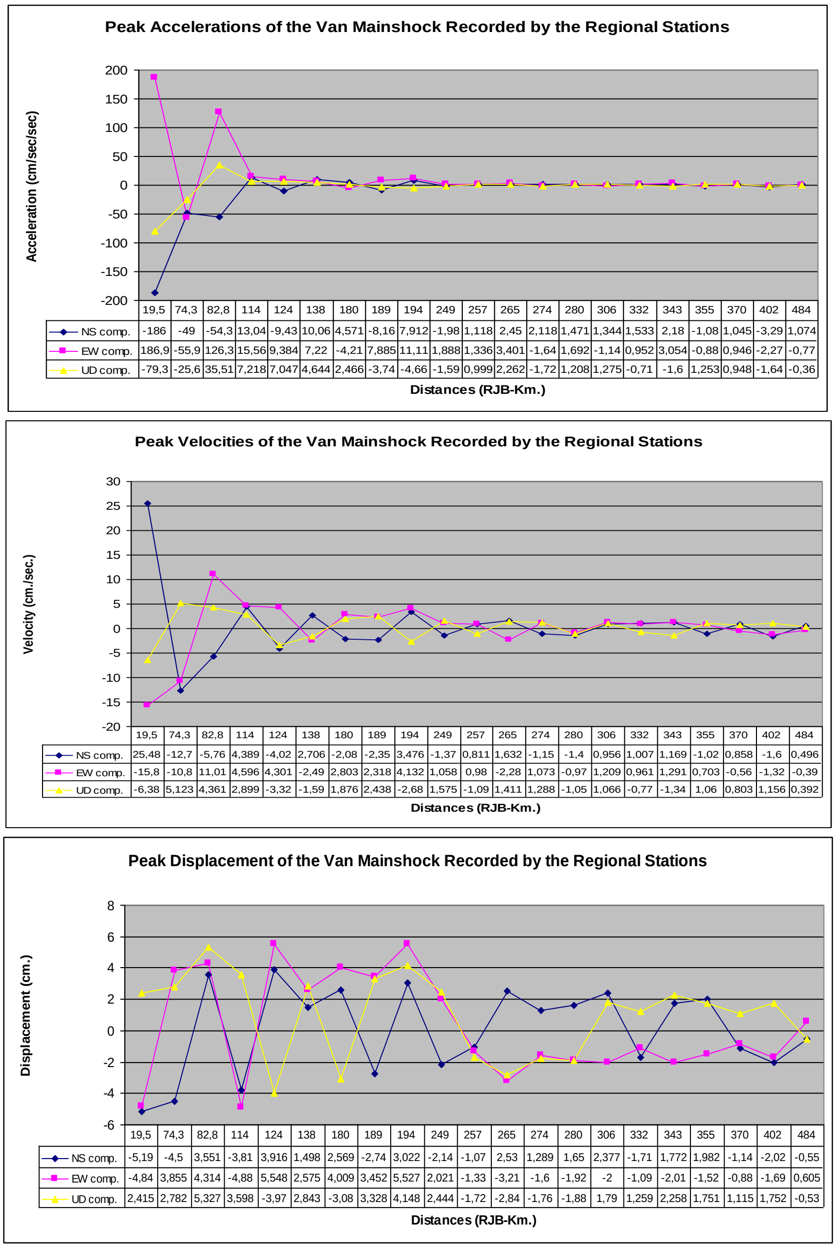


| | 19,5 | 74,3 | 82,8 | 114 | 124 | 138 | 180 | 189 | 194 | 249 | 257 | 265 | 274 | 280 | 306 | 332 | 343 | 355 | 370 | 402 | 484 |
|---|---|---|---|---|---|---|---|---|---|---|---|---|---|---|---|---|---|---|---|---|---|
| NS comp. | -186 | -49 | -54,3 | 13,04 | -9,43 | 10,06 | 4,571 | -8,16 | 7,912 | -1,98 | 1,118 | 2,45 | 2,118 | 1,471 | 1,344 | 1,533 | 2,18 | -1,08 | 1,045 | -3,29 | 1,074 |
| EW comp. | 186,9 | -55,9 | 126,3 | 15,56 | 9,384 | 7,22 | -4,21 | 7,885 | 11,11 | 1,888 | 1,336 | 3,401 | -1,64 | 1,692 | -1,14 | 0,952 | 3,054 | -0,88 | 0,946 | -2,27 | -0,77 |
| UD comp. | -79,3 | -25,6 | 35,51 | 7,218 | 7,047 | 4,644 | 2,466 | -3,74 | -4,66 | -1,59 | 0,999 | 2,262 | -1,72 | 1,208 | 1,275 | -0,71 | -1,6 | 1,253 | 0,948 | -1,64 | -0,36 |

| | 19,5 | 74,3 | 82,8 | 114 | 124 | 138 | 180 | 189 | 194 | 249 | 257 | 265 | 274 | 280 | 306 | 332 | 343 | 355 | 370 | 402 | 484 |
|---|---|---|---|---|---|---|---|---|---|---|---|---|---|---|---|---|---|---|---|---|---|
| NS comp. | 25,48 | -12,7 | -5,76 | 4,389 | -4,02 | 2,706 | -2,08 | -2,35 | 3,476 | -1,37 | 0,811 | 1,632 | -1,15 | -1,4 | 0,956 | 1,007 | 1,169 | -1,02 | 0,858 | -1,6 | 0,496 |
| EW comp. | -15,8 | -10,8 | 11,01 | 4,596 | 4,301 | -2,49 | 2,803 | 2,318 | 4,132 | 1,058 | 0,98 | -2,28 | 1,073 | -0,97 | 1,209 | 0,961 | 1,291 | 0,703 | -0,56 | -1,32 | -0,39 |
| UD comp. | -6,38 | 5,123 | 4,361 | 2,899 | -3,32 | -1,59 | 1,876 | 2,438 | -2,68 | 1,575 | -1,09 | 1,411 | 1,288 | -1,05 | 1,066 | -0,77 | -1,34 | 1,06 | 0,803 | 1,156 | 0,392 |

| | 19,5 | 74,3 | 82,8 | 114 | 124 | 138 | 180 | 189 | 194 | 249 | 257 | 265 | 274 | 280 | 306 | 332 | 343 | 355 | 370 | 402 | 484 |
|---|---|---|---|---|---|---|---|---|---|---|---|---|---|---|---|---|---|---|---|---|---|
| NS comp. | -5,19 | -4,5 | 3,551 | -3,81 | 3,916 | 1,498 | 2,569 | -2,74 | 3,022 | -2,14 | -1,07 | 2,53 | 1,289 | 1,65 | 2,377 | -1,71 | 1,772 | 1,982 | -1,14 | -2,02 | -0,55 |
| EW comp. | -4,84 | 3,855 | 4,314 | -4,88 | 5,548 | 2,575 | 4,009 | 3,452 | 5,527 | 2,021 | -1,33 | -3,21 | -1,6 | -1,92 | -2 | -1,09 | -2,01 | -1,52 | -0,88 | -1,69 | 0,605 |
| UD comp. | 2,415 | 2,782 | 5,327 | 3,598 | -3,97 | 2,843 | -3,08 | 3,328 | 4,148 | 2,444 | -1,72 | -2,84 | -1,76 | -1,88 | 1,79 | 1,259 | 2,258 | 1,751 | 1,115 | 1,752 | -0,53 |

Fig. 11 Peaks of acceleration, velocity and displacement time histories in vertical axis and distances ($r_{jb}$) of the recording stations in the horizontal axis with exact peak values tabulated below the graphic

parameters, material and representative models affect the structural safety assessment (Nemecek *et al*. 2013). Therefore in most cases it is impossible to regenerate three component recorded time histories with high correlation (i.e., it is impossible particularly for stations on the hanging wall site and footwall site with fault normal and fault parallel components). This fact has been also shown with the synthetics produced for the Van mainshocks. Earthquake demand from structure might be underestimated (e.g., 2.7 times at 0.5 sec structural period as given in Table 4) Damage or collapse in this case was inevitable. Thus, vulnerability analysis of a newly designed structure and assessment of retrofitting scheme strongly rely on seismotectonic facts and the derived parameters in the scope of engineering seismology.

As in the Van Earthquake, in order to see forward rupture directivity in reverse dip-slip events, rupture direction is expected to be aligned up on the fault plane and the slip vectors should point upwards as well (Poiata *et al*. 2012). It should not be forgotten that such conditions are not often met for the seismic events with normal faults. The effects occur mostly near the up dip projection on the surface or the surface rupture. Level of the dip angle changes the fault normal component. Values close to vertical dip angle, the strike-normal component can represent the fault-normal component but in case of low dip angles, the vertical component of recorded ground motion might be very strong and it may sufficiently represent the fault-normal component (Somerville *et al*. 1997). Therefore, a probable error (i.e., due to aleatoric or epistemic uncertainties) in the estimation of dip angle, horizontal and vertical components of recordings might be considered equally. Furthermore, coupled effect is also a reality in practice and should be considered in the design of structures.

The GMPEs relations will need to be applicable to a wider range of magnitudes and distances for the engineering practice. They may be incorporated with certain site categories and $V_{s30}$ (Averaged shear velocity value over the top 30 m) values to better account for site effects. Near-fault effects, fault rupture directivity effects, hanging wall and footwall effects might be incorporated in the available ground motion relations. Study on the regional recordings may give the possibility to provide local scaling for the aseismic design of engineering structures.

Distribution of the maximum displacements with almost stable values for the stations within the distances of 200 km for instance emphasizes the significance of the vertical component. Identically, such a reverse fault characteristic is also distinguished in vertical components of the regional elastic spectra. Due to the reverse faulting with large slip and dip angles, vertical displacements along with directivity and fault normal effects might significantly affect the engineering structures. Main reason of excessive damage in the town of Erciş can be attributed to these factors. Such effects should be considered in advance through the establishment of vertical design spectra.

The proposed spectral acceleration values in the TEC (2007) illustrate how well the recorded ground motions fitted to the estimates. The differences in these models are in the acceptable range. Such differences can be a result of using different databases, different statistical techniques for the regression models as well as the iterative algorithms.

Observed values inferred from the analysis of the strong ground motion data enable us get significant features of the earthquake source, forward directivity effects during the rupture process and local site effects. They were discussed in detail in the light of the Van Earthquake in this paper. Current conventions in seismic design and retrofitting of existing structures are also discussed to help further improvements of design and assessment of engineering structures for causative reverse faults in susceptible regions. This study also aimed to show the facts from different disciplines, since the systematic interpretation of such engineering effects is seen to be limited for the thrust fault causative earthquakes.

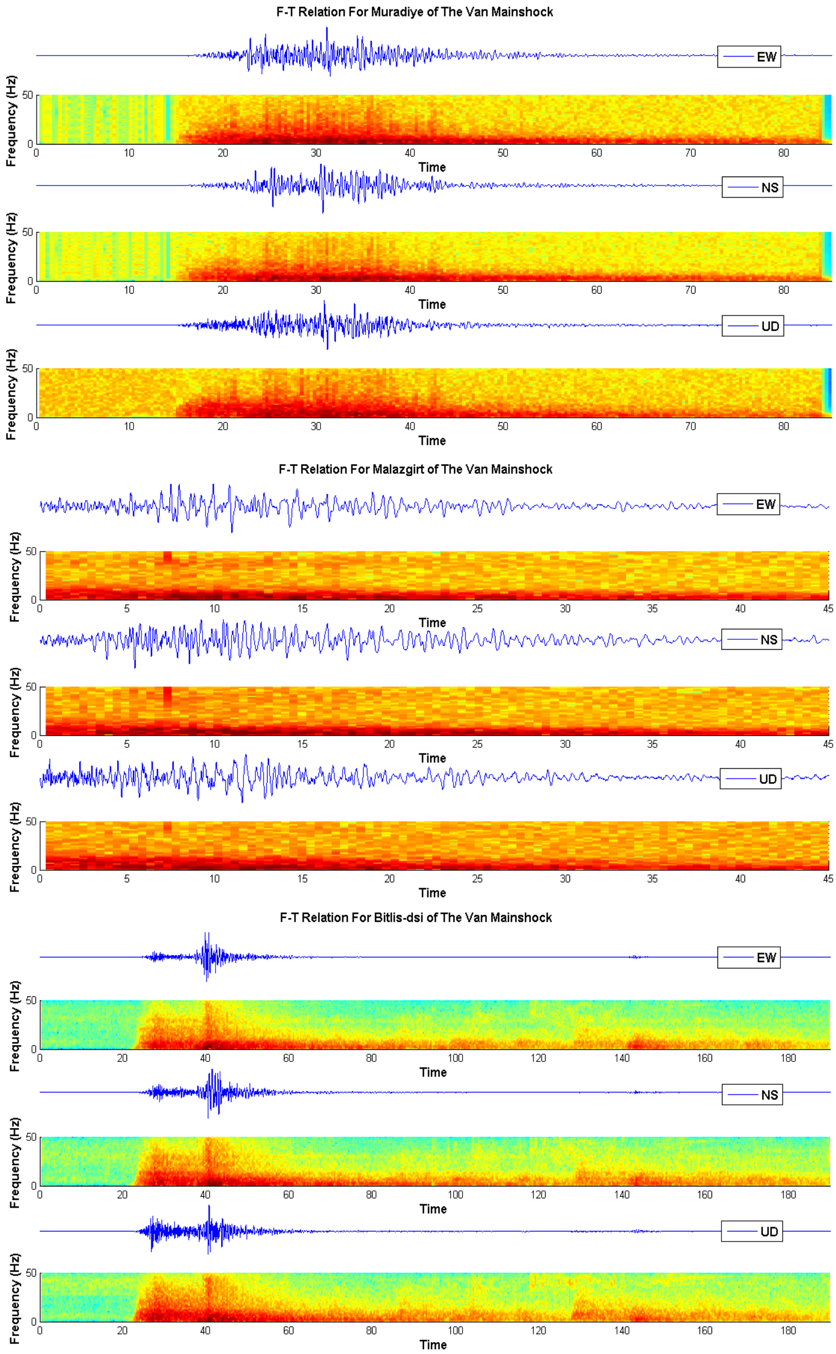


Fig. 12 Frequency-Time relations of the three closest stations (up):Muradiye, (middle) Malazgirt and (bottom) Bitlis) recorded main shock of the 23 October Van Earthquake and accelerations high pass filtered @ 2 Hz to remove site soil effects

Since the Muradiye station is located in the same distance to the epicenter, same ground motion levels can also be assumed for the cities of Van and Erciş. It should also be noted that Erciş city is located on the moving block of the rupture that may imply higher levels of ground motion than Van city. This fact is also manifested by the level of damage in Erciş, if compared with the damage documents of the city of Van.

In case of the magnitude distance models, as the confidence levels of the predictive models increase, peak ground motion predictions become consistent with the available measurements and such a consistency lets the engineers suggest the most probable peak values for districts with no instrumentation. As seen in the case of the city of Bitlis, effects of rupturing and directivity may increase the peak ground motion and should be considered by the predictive models.

Either damage or condition assessment of the structure through the nonlinear dynamic analyses may require new descriptive correlations between ground motion characteristics and structural response parameters. For instance, nonlinear responses of high-rise buildings was studied in cases of the characteristics of near and far field strong ground motions to find suitable parameters for magnitudes (Mw), faulting mechanisms and source to site distances with different soil conditions and site classes. It is found that the internal forces are increased by the increase of peak ground motion velocity and directivity effect increases the response when compared to their counterparts with no directivity effect (Engin 2014). In another study, Bülbül (2011) worked with near field strong ground motions and calculated displacement modification factor, which is the ratio between the maximum inelastic displacement and displacement calculated for the linear elastic response. They proposed an equation of mean factor as a function of normalized structural period by pulse period and strength reduction factor. Numerical examples have revealed that for structures whose period larger than 1 sec, the factor takes values between 1.1-3.6, where this value ($C_1$) is fixed to 1 in ASCE/SEI 41-06 (2007).

Better integration of multi-disciplinary hazard studies is necessary and would represent a great advance and contribution. Quantification of seismic design forces and currently employed methods in earthquake source simulation studies and assessment of the structural behavior may be ultimate goal to be carried out in cooperation by the recent advances in seismology and structural engineering. The Van Earthquake provided an opportunity to gain further insights into interactionally modified solutions from multidisciplinary studies.

## 8. Conclusions

This study focused on the effects of the seismology and earthquake physics on engineering design. Characteristics of the strong ground motion data recorded during the largest reverse mechanism earthquake in the instrumental period of Turkey were investigated. Theoretical and observational results suggest that there may be tolerable differences in simulations based on kinematic and dynamic properties of rupture and in numerical analysis due to inevitable assumptions and simplifications for the source mechanism models, which are not directly accessible to measurement. Effects of geologic conditions from the fault towards the site station should be represented good enough in order to estimate realistic time histories. Therefore strong ground motion with physics based solution of earthquake rupture and understanding of the earthquake process are very important central issue between aseismic design engineering and engineering seismology.

Significant engineering parameters were calculated and compared with GMPEs. Those equations may be incorporated with near-fault effects, fault rupture directivity effects, hanging wall and footwall effects and applicable to a wider range of magnitudes and distances for the engineering practice. Study on the regional recordings may give the possibility to provide local scaling for the aseismic design of engineering structures. Due to the reverse faulting with large slip and dip angles, vertical displacements along with directivity and fault normal effects might significantly affect the engineering structures. Main reason of excessive damage in the town of Erciş can be attributed to these factors. Such effects should be considered in advance through the establishment of vertical design spectra. Horizontal design spectra proposed by the TEC (2007) give safe spectral acceleration values when compared to those of the recorded ground motions. Significant features of the reverse faulting characteristics of the hanging wall and footwall and propagation effects in FN and FP directions as well as near and far site effects were discussed in the light of the Van main shock data. It has been shown that multi rupturing can also easily be seen on spectrograms portraying energy release throughout the record duration, particularly at three near stations.

Better integration of multi-disciplinary hazard studies is necessary and would represent a great advance and contribution. Quantification of seismic design forces and currently employed methods in earthquake source simulation studies and assessment of the structural behavior may be ultimate goal to be carried out in cooperation by the recent advances in seismology and structural engineering. The Van Earthquake provided an opportunity to gain further insights into interactionally modified solutions from multidisciplinary studies.

## Acknowledgements

Authors thank to the Kocaeli University for its support during site surveying. We would thank Dr. Frantisec Gallovic and Dr. Ayşegül Aşkan for supplying synthetic data of Muradiye station.

## References

Abrahamson, N.A. and Silva, W.J. (2008), “Summary of the Abrahamson and Silva NGA ground motion relations”, *Earthq. Spectra*, **24**(1), 45-66.

AFAD, Disaster and Emergency Management Presidency (DEMP) (2011), *Earthquake Report*.

Akoglu, A.M., Jonsson, S., Cakir, Z., Ergintav, S., Dogan, U., Feng, G. and Zabci, C. (2012), “The surface deformation and source parameters of the October 23rd, 2011, Mw 7.1 Van (Turkey) earthquake from InSAR, GPS and field observations”, *EGU General Assembly Conference Abstracts*, **14**, 12139.

ASCE/SEI 41-06 (2007), *Seismic Rehabilitation of Existing Buildings*, American Society of Civil Engineers, Virginia.

Ben-Zion, Y. and Sammis, C.G. (2003), “Characterization of fault zones”, *Pure Appl. Geophys.*, **160**(3-4), 677-715.

Boore, D.M. (1999), “Effect of baseline corrections on response spectra for two recordings of the 1999 Chi-Chi, Taiwan, Earthquake”, *USGS*, Open-File Report 99-545.

Boore, D.M. and Joyner, W.B. (1982), “The empirical prediction of ground motion”, *Bull. Seismol. Soc. Am*., **72**(6B), S43-S60.

Boore, D.M. and Atkinson, G.M. (2008), “Ground-motion prediction equations for the average horizontal component of PGA, PGV, and 5%-damped PSA at spectral periods between 0.01 s and 10.0 s”, *Earthq. Spectra*, **24**(1), 99-138.

Bülbül, Y.E. (2011), "Effect of near field ground motions on displacement amplification spectra in inelastic seismic performance evaluation", MSc., Thesis, Bogazici University, Turkey.

Campbell, K.W. and Bozorgnia, Y. (2008), "NGA ground motion model for the geometric mean horizontal component of PGA, PGV, PGD and 5% damped linear elastic response spectra for periods ranging from 0.01 to 10s", *Earthq. Spectra*, **24**(1), 139-171.

Chiou, B. and Youngs, R.R. (2008), "An NGA model for the average horizontal component of peak ground motion and response spectra", *Earthq. Spectra*, **24**(1), 173-215.

CEDIM, Forensic Earthquake Analysis Group (2011), *Comparing the current impact of the Van earthquake to past earthquakes in Eastern Turkey*, Report 4.

Derras, B., Bard, P.Y., Cotton, F. and Bekkouche, A. (2012), "Adapting the neural network approach to PGA prediction: an example based on the KiK-net data", *Bull. Seismol. Soc. Am.*, **102**(4), 1446-1461.

Dhakal, R.P. (2011), "Structural design for earthquake resistance: Past, present and future", *Canterbury Earthq. Roy. Comm*.

Doğan, B. and Karakaş, A. (2013), "Geometry of co-seismic surface ruptures and tectonic meaning of the 23 October 2011 M w 7.1 Van earthquake (East Anatolian Region, Turkey)", *J. Struct. Geo*., **46**, 99-114.

Dogan, U., Demir, D.Ö., Çakir, Z., Ergintav, S., Ozener, H., Akoğlu, A.M. and Reilinger, R. (2014), "Postseismic deformation following the Mw 7.2, 23 October 2011 Van earthquake (Turkey): Evidence for aseismic fault reactivation", *Geophys. Res. Lett*., **41**(7), 2334-2341.

Emre, O. *et al*. (2012), "Surface faulting associated with October 23, 2011 Van Earthquake (Mw 7.2) and shoreline uplifting of the Lake Van", *Proceedings of the 65th Geological Congress of Turkey*, April.

Emre, Ö., Tamer, Y., Duman, Selim, Özalp and Hasan, Elmaci (2011), "23 Ekim 2011 Van Depremi Saha Gözlemleri ve Kaynak Faya İlişkin Ön Değerlendirmeler", *Jeoloji Etütleri Dairesi, Yer Dinamikleri Araştırma ve Değerlendirme Koordinatörlüğü, Aktif Tektonik Araştırmaları Birimi*, Ankara. (in Turkish)

EMSC (2011), "23 October 2011 Van Earthquake", *Council of Europe, European-Mediter,* Seismological Centre, Special Earthquake Reports.

Engin, Serkan (2014), "Yakın Saha Kaynaklı Deprem Kayıtlarının Yüksek Yapıların Davranışına Etkisi-near field ground motion effects on the behavior of the high-rise buildings", Ph.D., Dissertaion, Kocaeli University, Kocaeli, Turkey.

Eric, J.F., Paul, R.L., Tuncay, T., Seda, Y.Ç. and Susan, E.O. (2013), "Fault-slip source models for the 2011 M 7.1 Van Earthquake in Turkey from SAR Interferometry, pixel offset tracking, GPS, and seismic waveform analysis", *Seismol. Res. Lett*., **84**(4), 579-593.

Gallovič, F., Ameri, G., Zahradník, J., Janský, J., Plicka, V., Sokos, E. and Pakzad, M. (2013), "Fault process and broadband ground-motion simulations of the 23 October 2011 Van (Eastern Turkey) Earthquake", *Bull. Seismol. Soc. Am*., doi: 10.1785/0120130044.

Glkan, P. (1978), *Engineering Report on the Muradiye-aldiran, Turkey, Earthquake of 24 November 1976*, National Academies.

Graizer, V. and Kalkan, E. (2004), "Ground motion attenuation model for peak horizontal acceleration from shallow crustal earthquakes", *Earthq. Spectra*, **23**(3), 585-613.

Hayes, G. (2011), "Finite fault model: updated result of the Oct 23, 2011 Mw 7.1 Eastern Turkey earthquake", http://earthquake.usgs.gov/earthquakes/eqinthenews/2011/usb0006bqc/finite_fault.php.

Heaton, T.H. (1992), "Overview of seismological methods for the synthesis of strong ground motion", *USGS*.

Husen, S. and Hardebeck, J.L. (2010), "Earthquake location accuracy", *Commun. Online Resource Stat. Seism. Anal*., **10**, doi:10.5078/corssa-55815573.

Irmak, T.S., Dogan, B. and Karakas, A. (2012), "Source mechanism of the 23 October, 2011, Van (Turkey) earthquake (*M*w=7.1) and aftershocks with its tectonic implications", *Earth Planet. Space*, **64**(11), 991-1003.

Iervolino, I., De Luca, F. and Cosenza, E. (2010), "Spectral shape-based assessment of SDOF nonlinear

response to real, adjusted and artificial accelerograms", *Eng. Struct.*, **32**(9), 2776-2792.
Kalkan, E. and Gülkan, P. (2004), "Site-dependent spectra derived from ground motion records in Turkey", *Earthq. Spectra*, **20**(4), 1111-1138.
Koçyiğit, A. (2013), "New field and seismic data about the intraplate strike-slip deformation in Van region, East Anatolian Plateau, E Turkey", *J. Asian Earth Sci*., **60**,586-605.
Matlab (2011), 6.1, The MathWorks Inc., Natick, MA, 2000.
McClusky, S., Balassanian, S., Barka, A., Demir, C., Ergintav, S., Georgiev, I. and Veis, G. (2000), "Global Positioning System constraints on plate kinematics and dynamics in the eastern Mediterranean and Caucasus", *J. Geophys. Res.: Solid Earth (1978-2012)*, **105**(B3), 5695-5719.
Mehdi, Ahmadizadeh (2007), "Real-time seismic hybrid simulation procedures for reliable structural performance testing", Ph.D., Dissertation, State University of New York, Buffalo.
Moro, M., Cannelli, V., Chini, M., Bignami, C., Melini, D., Stramondo, S., Saroli, M., Picchiani, M., Kyriakopoulos, C. and Brunori, C.A. (2014), "The October 23, 2011, Van (Turkey) earthquake and its relationship with neighbouring structures", Scientific reports, 4, doi: 10.1038/srep03959.
NEMC-KOERI (2011), "Report on the 23 October 2011", Bogazici University, Kandilli Observatory and Earthquake Research Institute, National Earthquake Monitoring Center (NEMC).
Němeček, J., Kralik, V. and Vondrejc, J. (2013), "Micromechanical analysis of heterogeneous structural materials", *Cement Concrete Compos.*, **36**, 85-92.
Okuldaş, C. and Ü ner, S. (2013), "Alaköy Fayı'nın Jeomorfolojik Özellikleri ve Tektonik Etkinliği (Van Gölü Havzası-Doğu Anadolu)", *Bulletin of the Earth Sciences Application and Research Centre of Hacettepe University*, **34**(3), 161-176. (in Turkish)
Ö zkaymak, Ç., Yürür, T. and Köse, O. (2004), "An example of intercontinental active collisional tectonics in the Eastern Mediterranean region (Van, Eastern Turkey)", *The 5th International Symposium on Eastern Mediterranean Geology*, Thessaloniki, T1-44.
PEER (2013), http://peer.berkeley.edu/peer_ground_motion_database/spectras/17691/edit.
Poiata, N., Miyake, H. and Koketsu, K. (2012), "Generation mechanism of near-fault ground motion pulses for dip-slip faulting", *15 WCEE*, Lisboa.
Sarno, L. Di., Yenidoğan, C. and Erdik, M. (2013), "Field evidence and numerical investigation of the Mw=7.1 October 23 Van, Tabanlı and the MW>5.7 November earthquakes of 2011", *Bull. Earthq. Eng*., doi: 10.1007/s10518-012-9417-0.
Smerzini, C., Galasso, C., Iervolino, I. and Paolucci, R. (2013), "Ground motion record selection based on broadband spectral compatibility", *Earthq. Spectra*, doi: 10.1193/052312EQS197M.
Şengör, A.M.C. and Kidd, W.S.F. (1979), "Post-collisional tectonics of the Turkish Iranian plateau and a comparison with Tibet", *Tectonophys.*, **55**(3), 361-376.
Somerville, P. and Abrahamson, N.A. (2000), *Prediction of ground motions for thrust earthquakes*, California Department of Conservation, Division of Mines and Geology, Office of Strong Motion Studies.
Somerville, P.G., Smith, N.F., Graves, R.W. and Abrahamson, N.A. (1997), "Modification of empirical strong ground-motion attenuation relations to include the amplitude and duration effect of rupture directivity", *Seismol. Res. Lett*., **68**(1), 199-222.
Turkish Earthquake Code (TEC) (2007), "Specifications for buildings to be built in seismic areas", Ministry of Public Works and Settlement, Ankara.
Ü ner, S., Yeşilova, Ç. and Yakupoğlu, T. (2012), "The traces of earthquake (seismites): Examples from Lake Van Deposits (Turkey)", *Earthquake Research and Analysis-Seismology, Seismotectonic and Earthquake Geology*, InTech, Rijeka, Croatia.
UBC 1997, International Conference of Building Officials (1997), "1997 Uniform Building Code Volume 2", International Conference of Building Officials Publication Department, Whittier, CA.
USGS (2011), "Report on earthquake activity -magnitude 7.1- Eastern Turkey", *Preliminary Earthquake Report*; *U.S. Geological Survey*, National Earthquake Information Center.

Utkucu Murat (2012), "23 October 2011 Van, Eastern Anatolia, earthquake (MW 7.1) and seismotectonics of Lake Van area", *J. Seismol*., **17**(2), 783-805.

Zengin, E. and Cakti, E. (2014), "Ground motion simulations for the 23 October 2011 Van, Eastern Turkey earthquake using stochastic finite fault approach", *Bull. Earthq. Eng.*, **12**(2), 627-646.

*SA*